Impact of DSI Implantable Devices on Single Photon Emission Computed Tomography (SPECT) Images

Two telemetry devices (Models L21 PTD and D70-PCTR) were attached to a cylindrical single photon emission computed tomography (SPECT) phantom and underwent a SPECT/CT scan on the IRF's Philips Precedence scanner. The phantom contained a uniform solution of the radioisotope ^{99m}Tc in water. Prior to the SPECT scan, a CT scan of the phantom with the attached telemetry devices was acquired. UUHR (ultra-ultra-high resolution) collimators were mounted to the two gamma cameras on the Precedence SPECT system. For the SPECT scan, the camera heads were rotated over 360 degrees to acquire a total of 128 views, each view acquired data for a duration of 30 seconds.

The Figures 1 and 2 below show an x-ray projection image of the phantom with the devices attached (dashed arrow: L21 PTD, solid arrow: D70-PCTR) and an example of one of the 128 raw SPECT projection images with no attenuation correction. Figure 2 illustrates the extent to which the devices attenuate the 140 keV gamma rays emitted by the ^{99m}Tc isotope.

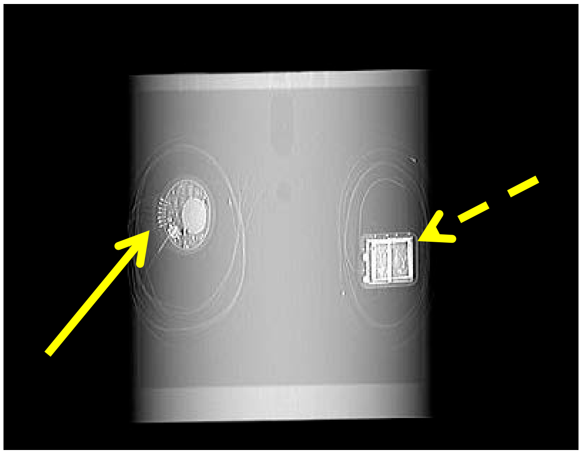

Figure 1: X-ray image of cylindrical phantom with devices.

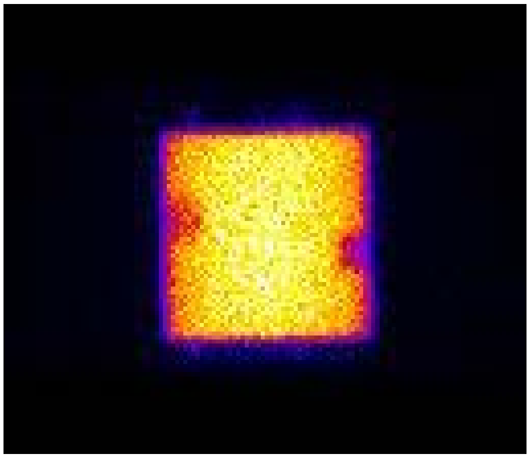

Figure 2 Uncorrected SPECT projection image of phantom

Cross-sectional CT images through the phantom at the locations of the circular D70-PCTR device and the rectangular L21 PTD device are shown below in Figures 3 and 4. The brightness of the telemetry devices in the CT slices is a result of their high electron density and subsequent x-ray attenuation. To a good approximation, the average energy in an x-ray beam corresponds to half of the peak tube voltage (kVp). For the images shown below, kVp = 120 keV and the average x-ray energy was about 60 keV.

The ^{99m}Tc gamma rays have an energy of 140 keV, considerably higher than the x-ray energy. In order to create an attenuation map for the SPECT attenuation correction, the CT numbers (in Hounsfield units, obtained at approximately 60 keV) have to be transformed into linear attenuation coefficients at 140 keV. This process requires some knowledge of the elemental composition of the material involved. It is common for reconstruction software to assume that the elemental composition of objects in the CT image is either soft tissue (i.e. water) or bone (i.e. calcium). Clinically speaking, this is a good assumption. However, the metallic contents of the telemetry devices will lead to an overestimation of the true attenuation at 140 keV. In turn, this should lead to an overestimation of the activity level in the phantom near the sites where the test devices are attached.

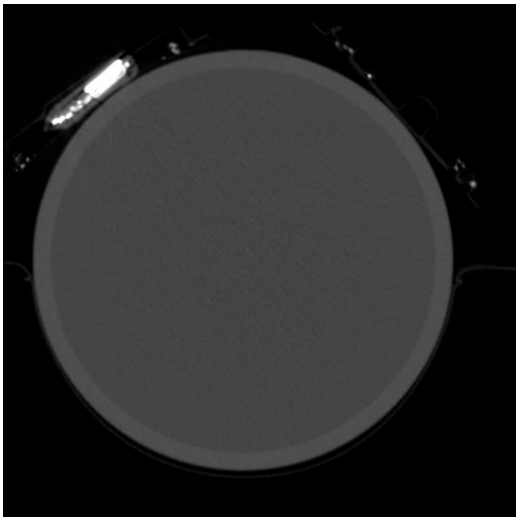

Figure 3: CT slice through phantom and D70-PCTR.

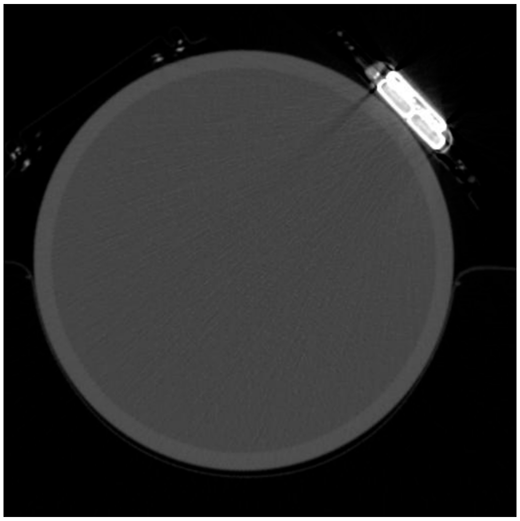

Figure 4 CT slice through phantom and L21-PTD

Results and Conclusion

SPECT images were reconstructed from the 128 projections. The individual projection images were corrected for field uniformity, radioactive decay during the approximately 65 minute scan, scattered radiation and attenuation. Two different image reconstruction algorithms were used and evaluated, both falling into the class of iterative expectation maximization (EM) algorithms. The first one is the widely used 3D-OSEM algorithm (where OS stands for ordered subsets) and the second one is Philips recommended ASTONISH algorithm which is also a form of 3D-OSEM but uses a proprietary resolution kernel. Both algorithms support the correction for scatter and attenuation based on the CT-scan acquired prior to the SPECT scan.

Two SPECT slices each from the 3D-OSEM and the ASTONIGH image reconstructions are shown in Figure 5 and 6, respectively. The locations of the SPECT slices match those of the CT slices shown in Figures 3 and 4. The two reconstruction algorithms exhibit different signal/noise characteristics as a function of input parameters, e.g. number of iterations and subsets. In order to ensure a fair comparison between the two algorithms, the number of iterations and subsets for each algorithm were adjusted to produce a comparable level of noise in both types of images.

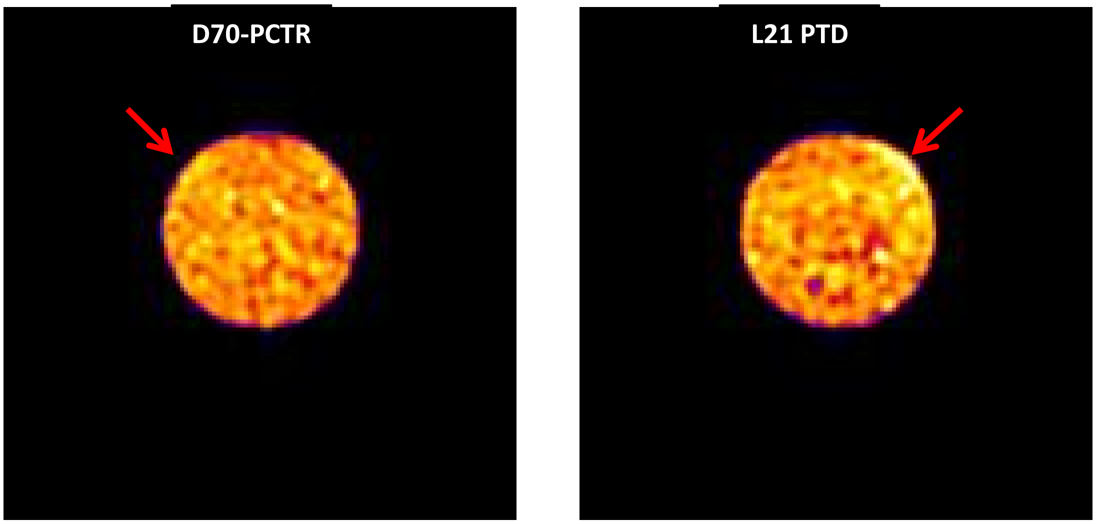

Figure 5: SPECT images reconstructed with 3D-OSEM showing D70-PCTR (left) and L21 PTD (right). Brightness levels adjusted to min=600 and max=1600.

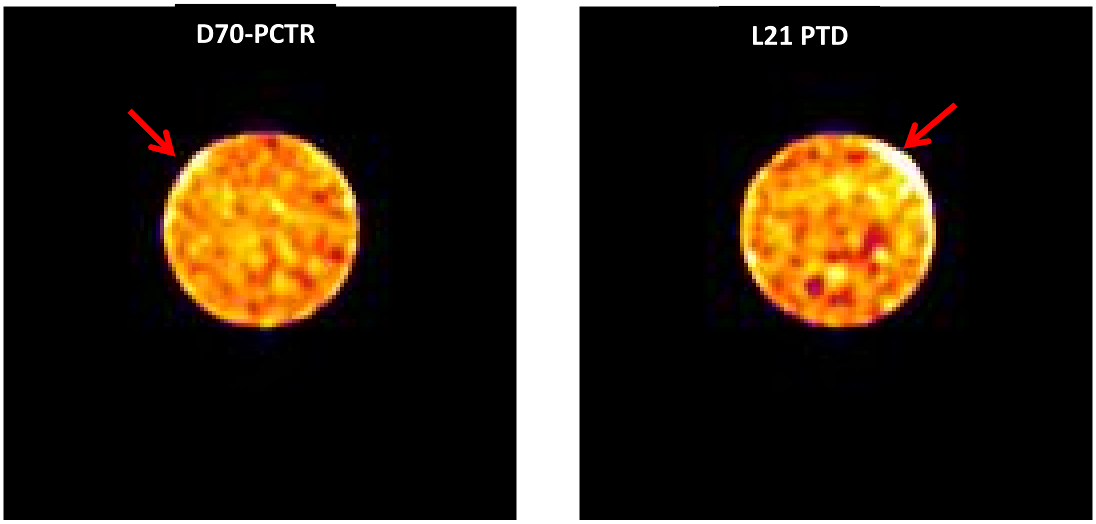

Figure 6: SPECT images reconstructed with Philips' ASTONISH algorithm showing D70-PCTR (left) and L21-PTD (right). Image brightness adjusted to same levels as in Figure 5.

In the Figures 5 and 6, red arrows point to brightness enhancements that correspond to the sites where the devices were attached. As discussed above, these enhancements are caused by a local over-correction for attenuation by the attached objects. Further analysis revealed that the amount of enhancement depends on the type of device and, surprisingly, also on the type of reconstruction algorithm. Table 1 below summarizes the numerical results.

Table 1: Brightness enhancement near site of attached telemetry devices in SPECT images reconstructed with the 3D-OSEM and the ASTONISH algorithm. Numbers represent percent change over the mean brightness in the SPECT phantom.

	D70-PCTR	L21 PTD
3D-OSEM	+13%	+21%
ASTONISH	+26%	+54%

Our investigation revealed that the presence of the two telemetry devices can lead to local brightness distortions in the SPECT images. With the Philips recommended ASTONISH reconstruction, local activity can be overestimated by up to 54%. With the standard 3D-OSEM reconstruction, the overestimation is substantially less (up to 21%). It is not clear why the two algorithms perform so differently. For this reason, it is impossible to predict how other SPECT systems would respond to the presence of the telemetry devices. However, we believe that the root cause for these artifacts is an overcorrection for attenuation. It seems worthwhile to investigate potential improvements to the attenuation correction process. One such possibility could consist of imposing an upper limit to the numbers in the CT image (or in the attenuation map) that corresponds to bone tissue or a similar value that minimizes the distortion. This “quick-fix” could be fairly easy to implement. Another possibility is to use the dual-energy CT scan technique that allows, in principle, to determine the elemental composition of the object and, thus, allows the construction of more accurate attenuation maps than the ones currently in use. This, however, will require a bigger effort to implement.